Apelin promotes RANKL-mediated osteoclastogenesis by activating MAPK and NF-κB pathways

YU-HAN WANG[1,2*], YU-YING WU[3,4*], CHUN-HAO TSAI[5,6], YI-CHIN FONG[5-7], CHIH-YUAN KO[6], HSIEN-TE CHEN[5,6], YAT-YIN LAW[3,4] and CHIH-HSIN TANG[1,8,9]

[1]Department of Pharmacology, School of Medicine, China Medical University, Taichung 404328, Taiwan, R.O.C.; [2]Institute of Medicine, Chung Shan Medical University, Taichung 402306, Taiwan, R.O.C.; [3]Department of Orthopedics, Chung Shan Medical University Hospital, Taichung 402306, Taiwan, R.O.C.; [4]School of Medicine, Chung Shan Medical University, Taichung 402306, Taiwan, R.O.C.; [5]Department of Sports Medicine, College of Health Care, China Medical University, Taichung 402306, Taiwan, R.O.C.; [6]Department of Orthopedic Surgery, China Medical University Hospital, Taichung 404327, Taiwan, R.O.C.; [7]Department of Orthopedic Surgery, China Medical University Beigang Hospital, Yunlin County 651012, Taiwan, R.O.C.; [8]Department of Medical Laboratory Science and Biotechnology, Asia University, Taichung 41354, Taiwan, R.O.C.; [9]Chinese Medicine Research Center, China Medical University, Taichung 404328, Taiwan, R.O.C.

Received July 8, 2025; Accepted October 15, 2025

DOI: 10.3892/mmr.2025.13751

Abstract. The regulation of bone mass relies on a dynamic interplay between bone-forming osteoblasts and bone-resorbing osteoclasts. Imbalances in this regulatory system favor bone resorption and are implicated in the development of osteolytic disorders such as osteoporosis. Although current treatments targeting osteoclast activity are effective, safety concerns remain a notable limitation. As a multifunctional adipokine, apelin (APLN) serves a role in angiogenesis and metabolic regulation. However, to the best of our knowledge, its involvement in osteoclast differentiation has not yet been characterized. The present study thus examined the effects of APLN on osteoclastogenesis using a murine-macrophage model stimulated with receptor activator of NF-κB ligand (RANKL). The results revealed that APLN augmented RANKL-induced osteoclast differentiation, promoting the formation of tartrate-resistant acid phosphatase-positive multinucleated cells and the development of organized F-actin rings. Transcriptome analyses of a public dataset confirmed the temporal upregulation of osteoclast-related genes under RANKL stimulation. It was further discovered that co-treatment with APLN and RANKL significantly enhanced the expression of these osteoclast-specific markers. APLN co-treatment with RANKL upregulated the ERK, JNK, p38 and NF-κB signaling pathways, and this activation was effectively attenuated by specific pathway inhibitors. In conclusion, these findings identified APLN as an enhancer of RANKL-dependent osteoclast differentiation and signaling, suggesting that the modulation of APLN activity may provide a promising strategy for controlling excessive bone resorption in skeletal diseases.

Correspondence to: Professor Chih-Hsin Tang, Department of Pharmacology, School of Medicine, China Medical University, 91 Xueshi Road, North, Taichung 404328, Taiwan, R.O.C.
E-mail: chtang@mail.cmu.edu.tw

Dr Yat-Yin Law, Department of Orthopedics, Chung Shan Medical University Hospital, 110 Sector 1, Jianguo North Road, South, Taichung 402306, Taiwan, R.O.C.
E-mail: andrewlaw@seed.net.tw

*Contributed equally

Key words: apelin, osteoclast, receptor activator of NF-κB ligand, bone resorption, MAPK pathway, NF-κB pathway

Introduction

Bone homeostasis is maintained through the dynamic balance between osteoblast-mediated bone formation and osteoclast-mediated bone resorption (1). The disruption of this balance results in bone loss, contributing to a variety of skeletal disorders, including osteoporosis, rheumatoid arthritis, periodontitis and bone metastases (2-4). Among these disorders, osteoporosis is the most prevalent, particularly in aging populations, and is marked by decreased bone mass and a higher risk of fractures (5). Current therapeutic strategies for bone loss primarily target osteoclast function, including bisphosphonates, denosumab and selective estrogen receptor modulators (SERMs) (6). However, these treatments are often associated with side effects, including osteonecrosis of the jaw, atypical femoral fractures and impaired bone remodeling (7), highlighting the need for the identification of novel therapeutic targets with improved safety profiles.

Bone loss typically results from dysregulated osteoclastogenesis and increased osteoclast-mediated resorption. Osteoclasts are multinucleated cells derived from macrophage progenitors, which are important for physiological bone remodeling and pathological bone resorption (8). The differentiation and activity of osteoclasts are tightly regulated by a range of signaling molecules, among which receptor activator

of NF-κB ligand (RANKL) serves a central role (9). The binding of RANKL to receptor activator of NF-κB (RANK) on osteoclast precursors initiates multiple intracellular signaling cascades, including the MAPK and NF-κB pathways, which converge to activate transcription factors such as nuclear factor of activated T-cells 1 (NFATc1) and c-Fos (10). These events drive the fusion of mononuclear precursors into multinucleated osteoclasts capable of bone resorption. Given the central role of RANKL signaling in osteoclastogenesis, the inhibition of its downstream pathways has been considered a promising therapeutic approach for mitigating pathological bone loss.

Apelin (APLN) is an endogenous peptide and an adipokine implicated in various physiological processes (11). APLN exerts its effects through binding to the G protein-coupled receptor APLN receptor, and is known to regulate angiogenesis, energy homeostasis and cardiovascular function (12-14). For example, studies have demonstrated that APLN promotes the expression of hypoxia-inducible factor-1, VEGF and VEGF receptor 2, thereby enhancing endothelial cell proliferation and migration, and ultimately facilitating new blood vessel formation (12,15). APLN has also been reported to promote inflammatory responses by upregulating the expression of IL-1β in human synovial fibroblasts, an effect linked to microRNA (miRNA)-144-3p suppression, and activation of the PI3K and ERK signaling pathways (16). Emerging evidence has indicated that adipokines may influence bone metabolism. Leptin is known to influence bone formation through central and peripheral pathways (17), whereas adiponectin has been demonstrated to inhibit osteoclastogenesis and enhance osteoblast differentiation (18). Previous evidence has suggested a regulatory role for APLN in skeletal homeostasis, as APLN deficiency in mice leads to increased trabecular and cortical bone mass along with elevated osteoblast activity and bone formation. APLN promotes osteoblast proliferation but does not enhance mineralized nodule formation, suggesting a potential disruption of osteoblast maturation. These findings indicate that APLN may act as an antianabolic factor and contribute to bone metabolic imbalance (19). However, the potential influence of APLN on osteoclast lineage cells, which are primarily responsible for bone resorption, remains ambiguous. Elucidating whether APLN contributes to osteoclast formation and function is important for understanding its broader role in bone remodeling.

To address this, the present study examined the effects of APLN on RANKL-induced osteoclastogenesis using the murine RAW264.7 cell model. Specifically, the present study evaluated the role of APLN in promoting osteoclast differentiation, regulating cytoskeletal organization and modulating intracellular signaling pathways associated with osteoclast activation. The results of the current study may provide new perspectives on the involvement of APLN in bone metabolism and suggest that the inhibition of APLN may represent a novel therapeutic strategy for suppressing excessive bone resorption in osteolytic diseases.

Materials and methods

Materials and reagents. Recombinant APLN was purchased from MyBiosource, Inc., and recombinant RANKL was obtained from PeproTech, Inc. (Thermo Fisher Scientific, Inc.). The ERK inhibitor FR180204, and antibodies against phosphorylated (p)-ERK (cat. no. sc-7383), p-JNK (cat. no. sc-6254) and p-p38 (cat. no. sc-166182), and total ERK (cat. no. sc-1647), JNK (cat. no. sc-7345) and p38 (cat. no. sc-7972) were acquired from Santa Cruz Biotechnology, Inc. The JNK inhibitor SP600125 was purchased from Enzo Life Sciences, Inc. whereas the p38 inhibitor SB203580 and NF-κB inhibitor pyrrolidinedithiocarbamate ammonium (PDTC) were obtained from MilliporeSigma.

Antibodies against IKK (cat. no. GTX52348), IκB (cat. no. GTX110521), p65 (cat. no. GTX102090) and β-actin (1:10,000; cat. no. GT5512) were purchased from GeneTex International Corporation. Antibodies for p-IKK (cat. no. 2697S) were from Cell Signaling Technology, Inc., antibodies for p-IκB (cat. no. sc-8404) were obtained from Santa Cruz Biotechnology, Inc. and antibodies targeting p-p65 (cat. no. AP0124) were obtained from ABclonal Biotech Co., Ltd.

Cells and cell cultures. RAW264.7 murine macrophage-like cells were purchased from the American Type Culture Collection, and were maintained in Dulbecco's modified Eagle's medium (DMEM; Gibco, Thermo Fisher Scientific, Inc.) supplemented with 10% characterized fetal bovine serum (FBS; HyClone™; Cytiva) and the standard antibiotics penicillin/streptomycin (100 IU/ml). Cells were maintained at 37˚C in a 5% CO_2 humidified incubator.

Osteoclast differentiation and treatment. RAW264.7 cells ($2x10^3$/well) were seeded into 24-well plates and cultured in DMEM supplemented with 10% FBS. For osteoclast differentiation, cells were treated with RANKL (50 ng/ml), either alone or in combination with APLN (1, 3 or 10 ng/ml), for 5 days at 37˚C with 5% CO_2. For the neutralization group, cells were pre-incubated with APLN antibody (1 μg/ml; cat. no. NBP3-12282; Novus Biologicals; Bio-Techne) for 30 min before the addition of RANKL and APLN. The culture medium was refreshed every 2 days. The optimal concentration of APLN (10 ng/ml) was determined from a preliminary dose response assay in RAW264.7 cells, in which this concentration induced maximal osteoclast differentiation without affecting cell viability. A previous study also reported that pyroglutamyl-APLN-13, a distinct peptide fragment of the APLN molecule, at the same concentration modulated macrophage functions in RAW264.7 cells (20).

For tartrate-resistant acid phosphatase (TRAP) staining, cells were fixed with 10% paraformaldehyde for 5 min at room temperature, followed by incubation with the TRAP Staining Kit (cat. no. PMC-AK04-COS; Cosmo Bio Co., Ltd.) at 37˚C for 60 min. TRAP staining was conducted using a commercial TRAP kit (Cosmo Bio Co., Ltd.), and TRAP-positive multinucleated cells, defined as cells containing three or more nuclei, were identified by light microscopy (KimForest Enterprise Co., Ltd.). Images were analyzed using ImageJ software (v1.8.0; National Institutes of Health). The TRAP-positive area in each well was quantified and mean values were calculated from three independent experiments. For each well, images from three randomly selected microscopic fields were captured and averaged. For comparative analysis, TRAP-positive areas were normalized to the RANKL-only group (100%), which

served as the positive control. All images include a scale bar of 100 μm.

For pathway inhibition, RAW264.7 cells ($1x10^5$/well) were seeded into 6-well plates and pretreated with specific pathway inhibitors for 30 min at 37˚C with 5% CO_2 before stimulation with RANKL (50 ng/ml) + APLN (10 ng/ml) for 5 days. The culture medium was refreshed every 2 days. The final inhibitor concentrations were as follows: ERK inhibitor FR180204 (10 μM), JNK inhibitor SP600125 (10 μM), p38 inhibitor SB203580 (10 μM) and NF-κB inhibitor PDTC (20 μM).

Immunofluorescence staining. RAW264.7 cells ($2x10^3$/well) were seeded directly into 24-well plates and treated with RANKL (50 ng/ml) with or without APLN (10 ng/ml) for 5 days at 37˚C. Following treatment, the cells were fixed with 3.7% paraformaldehyde for 15 min and permeabilized with 0.5% Triton X-100 for 10 min at room temperature. F-actin staining was performed by incubating the cells overnight at 4˚C with Alexa Fluor 488-conjugated phalloidin (cat. no. A12379; Thermo Fisher Scientific, Inc.; diluted 1:300 in PBS). Nuclei were counterstained with DAPI. Fluorescence images were captured using an ImageXpress Pico imaging system (Molecular Devices, LLC). The F-actin ring area was quantified using ImageJ software (v1.8.0) and expressed relative to the RANKL-only group. All images include a scale bar of 100 μm.

Transcriptome analysis. RNA-sequencing (RNA-seq) data from the GSE21639 dataset were downloaded from the Gene Expression Omnibus database (https://www.ncbi.nlm.nih.gov/geo/query/acc.cgi?acc=GSE21639) (21). Differentially expressed genes (DEGs) between control and RANKL-treated RAW264.7 cells on days 2 and 5 were identified using GEO2R (https://www.ncbi.nlm.nih.gov/geo/info/geo2r.html) (22), applying a threshold of absolute $\log_2$(fold change)≥2 and an adjusted P-value≤0.05. Boxplot and uniform manifold approximation and projection (UMAP) analyses were performed using R software (version 4.2.2) (https://cran.r-project.org/bin/windows/base/old/4.2.2/) with the GEOquery (https://bioconductor.org/packages/release/bioc/html/GEOquery.html), limma (https://bioconductor.org/packages/release/bioc/html/limma.html) and UMAP packages (https://cran.r-project.org/web/packages/umap/index.html) to evaluate the quality of the GSE21639 dataset, and to confirm consistent overall gene expression distributions and clustering patterns. Gene Ontology (GO) and Kyoto Encyclopedia of Genes and Genomes (KEGG) pathway enrichment analyses were performed using the Database for Annotation, Visualization and Integrated Discovery v.6.8 (https://davidbioinformatics.nih.gov) (23).

Reverse transcription-quantitative PCR (RT-qPCR). Cellular RNA was obtained from RAW264.7 cells using TRIzol® reagent according to the manufacturer's instructions (cat. no. 12183555; Invitrogen; Thermo Fisher Scientific, Inc.), and cDNA was generated using the M-MLV Reverse Transcriptase Kit (Invitrogen; Thermo Fisher Scientific, Inc.) in accordance with the manufacturer's recommendation. SYBR Green-based qPCR was performed using SYBR™ Green PCR Master Mix (Applied Biosystems; Thermo Fisher Scientific, Inc.) on a StepOnePlus Real-Time PCR System (Applied Biosystems; Thermo Fisher Scientific, Inc.), with GAPDH as the reference gene. The cycling conditions were as follows: Initial denaturation at 95˚C for 20 sec, followed by 40 cycles at 95˚C for 3 sec and 60˚C for 30 sec. Subsequently, a melt curve analysis was performed. Expression levels were normalized and calculated using the $2^{-\Delta\Delta Cq}$ method (24). The mouse primer sequences used were as follows: Cathepsin K (CTSK), forward 5'-AGTAGCCACGCTTCCTATCC-3', reverse 5'-CCATGGGTAGCAGCAGAAAC-3'; acid phosphatase 5, tartrate resistant (ACP5), forward 5'-ATGGGCGCTGACTTCATCAT-3', reverse 5'-GGTCTCCTGGAACCTCTTGT-3'; matrix metalloproteinase 9 (MMP9), forward 5'-GGACCCGAAGCGGACATTG-3', reverse 5'-CGTCGTCGAAATGGGCATCT-3'; NFATc1, forward 5'-GACCCGGAGTTCGACTTCG-3', reverse 5'-TGACACTAGGGGACACATAACTG-3'; and GAPDH, forward 5'-TGTGTCCGTCGTGGATCTGA-3', reverse 5'-TTGCTGTTGAAGTCGCAGGAG-3.

Western blot analysis. RAW264.7 cells were lysed in RIPA buffer (cat. no. P0013; Beyotime Biotechnology) containing protease and phosphatase inhibitors. Protein levels were measured by BCA assay, and total proteins (30 μg) were separated by SDS-PAGE on 10% gels and were subsequently transferred to PVDF membranes. Blocking was performed with 5% non-fat milk for 1 h at room temperature, followed by overnight incubation with primary antibodies (1:1,000 for p-proteins and 1:2,000 for total proteins) at 4˚C, and detection with HRP-conjugated secondary antibodies (goat anti-rabbit IgG, cat. no. sc-2004 for IKK, IκB, p65, p-IKK, p-IκB, and p-p65; 1:2,000; goat anti-mouse IgG, cat. no. sc-2302 for p-ERK, p-JNK, p-p38, ERK, JNK, and p38; 1:2,000; both from Santa Cruz Biotechnology, Inc.) for 1 h at room temperature, followed by western chemiluminescent HRP substrate (ECL) detection (MilliporeSigma). Band intensities were measured using ImageJ software (v1.8.0).

NF-κB reporter assay. NF-κB luciferase reporter assays were conducted using the pNF-κB-Luc plasmid from the NF-κB cis-Reporting System (cat. no. 219077; Agilent Technologies, Inc.). The vector contains five tandem NF-κB response elements upstream of a minimal promoter driving luciferase expression. RAW264.7 cells were transfected with NF-κB luciferase constructs using Lipofectamine® 2000 (Invitrogen; Thermo Fisher Scientific, Inc.) and treated with RANKL (50 ng/ml) or RANKL (50 ng/ml) + APLN (10 ng/ml) 24 h after transfection for an additional 24 h at 37˚C with 5% CO_2. Luciferase activity was assessed using the Dual-Luciferase Reporter assay (Promega Corporation) and measured with a Fluoroskan Ascent Microplate Luminometer (Thermo Fisher Scientific, Inc.). The relative NF-κB luciferase activity was normalized to the control group and expressed as a percentage of the control value (% of control).

Statistical analysis. All experiments were performed in triplicate. Statistical analysis was performed using one-way ANOVA followed by the Bonferroni post hoc test for pairwise comparisons between selected groups. All data are presented as the mean ± standard deviation, and $P<0.05$ was considered to indicate a statistically significant difference. Analyses were performed using GraphPad Prism 9.0 (Dotmatics).

Results

APLN promotes RANKL-induced osteoclast differentiation and enhances F-actin ring formation. The ability of RANKL to induce osteoclast differentiation in RAW264.7 cells has been extensively validated *in vitro* (25). In the present study, RAW264.7 cells were stimulated with RANKL (50 ng/ml) in the presence of increasing concentrations of APLN (1, 3 or 10 ng/ml) for 5 days to assess whether APLN modulated osteoclastogenesis. TRAP staining revealed a marked increase in the size of multinucleated osteoclasts in cells co-treated with APLN and RANKL compared with RANKL alone (Fig. 1A). By contrast, APLN treatment alone did not induce osteoclast formation (Fig. 1A), indicating that APLN enhanced RANKL-induced osteoclastogenesis as opposed to initiating the differentiation process independently.

In addition, quantitative analysis of the mature osteoclast area supported that APLN co-treatment with RANKL significantly increased the osteoclast area in a concentration-dependent manner, with the 10 ng/ml treatment group having exhibited the most pronounced effect (Fig. 1B). Furthermore, to functionally validate whether the pro-osteoclastic effect of APLN was reversible, an APLN-neutralizing antibody was co-administered together with RANKL and APLN (10 ng/ml). TRAP staining results demonstrated that the enhanced osteoclast formation observed in the APLN + RANKL group was markedly attenuated by the addition of APLN antibody (Fig. 1A). Quantitative analysis showed a significant reduction in osteoclast area, not only reversing the APLN-mediated enhancement but further suppressing osteoclastogenesis, resulting in an osteoclast area lower than that induced by RANKL alone (Fig. 1B). These findings suggested that APLN may serve an important modulatory role in osteoclast differentiation and that its effects could be effectively neutralized by targeted-antibody blockade.

To further investigate whether APLN also affected the functional activity of mature osteoclasts, the present study evaluated F-actin ring formation using immunofluorescence staining, which specifically reflects cytoskeletal organization and the resorptive capacity of osteoclasts. RAW264.7 cells treated with RANKL alone exhibited F-actin ring formation. By contrast, co-treatment with APLN led to a concentration-dependent increase in the size of F-actin rings (Fig. 2A). Quantitative analysis revealed that the F-actin ring area was significantly greater in the cells co-treated with RANKL and APLN, particularly in the cells treated with the 10 ng/ml APLN, compared with the RANKL-only group (Fig. 2B). These findings allowed for the comprehensive assessment of the functional activity of osteoclasts in the presence of APLN and provided further insight into its role in RANKL-mediated osteoclastogenesis and bone resorption.

APLN facilitates RANKL-induced osteoclastogenic gene expression. Previous research has demonstrated that osteoclast marker genes such as ACP5, CTSK, MMP9 and NFATc1 are upregulated during osteoclast differentiation (26). To support this observation, the present study analyzed RNA-seq data from the GSE21639 dataset, which included RAW264.7 cells treated with or without RANKL for 2 and 5 days. The heatmap with hierarchical clustering revealed increased expression of ACP5, CTSK, MMP9 and NFATc1 in RANKL-treated groups compared with that in the control groups. Both control and RANKL groups clustered tightly within their respective branches, indicating high intra-group consistency and clear separation between conditions (Fig. 3A). As additional evidence of dataset quality, boxplot and UMAP analyses showed consistent expression distributions without outliers and clustering patterns aligned with experimental conditions (Fig. 3B), indicating effective normalization, high reproducibility and biological relevance. Further quantification revealed that the ACP5, CTSK and MMP9 levels were significantly elevated on both day 2 and 5 following RANKL stimulation compared with those in the control group. However, NFATc1 exhibited a significant increase in expression in the RANKL-treated group on day 5 only (Fig. 3C). The present study also validated the findings of the transcriptome analysis and assessed the effects of APLN on osteoclast-specific gene expression in RAW264.7 cells. RT-qPCR analysis demonstrated that co-treatment with RANKL and APLN increased ACP5, CTSK, MMP9 and NFATc1 mRNA expression relative to RANKL alone, showing a dose-dependent response, with statistical significance observed only at 10 ng/ml APLN (Fig. 3D). Notably, APLN treatment alone had no notable effect. These findings indicated that APLN may facilitate RANKL-induced osteoclastogenic gene expression, thereby supporting its functional role as a positive regulator of osteoclast differentiation.

Transcriptome enrichment analysis reveals osteoclast-related pathways activated by RANKL. To provide further mechanistic insights into the biological processes and signaling pathways involved in APLN-enhanced osteoclastogenesis, the present study analyzed DEGs using RNA-seq data from the GSE21639 dataset. This dataset contains data on RAW264.7 cells cultured with RANKL for 5 days. DEGs were defined using thresholds of $|\log_2(\text{fold change})|>2$ and $P<0.05$. GO enrichment analysis revealed that upregulated DEGs were significantly associated with biological processes relevant to osteoclast activity, including 'osteoclast differentiation', 'regulation of bone remodeling' and 'regulation of bone resorption' (Fig. 4A). Furthermore, KEGG pathway analysis demonstrated significant enrichment in key signaling cascades, including the 'MAPK signaling pathway' and 'NF- kappa B signaling pathway' (Fig. 4B). These findings highlighted the involvement of osteoclast-related biological processes and signaling pathways in RANKL-induced differentiation.

APLN promotes RANKL-mediated osteoclast differentiation through MAPK and NF-κB signaling pathways. Given the enrichment of MAPK and NF-κB pathways observed in transcriptome analysis, the present study then investigated whether these pathways contributed to the pro-osteoclastogenic effects of APLN. Western blot analysis revealed that co-treatment with APLN and RANKL markedly enhanced the phosphorylation of ERK, JNK and p38 compared with RANKL treatment alone (Fig. 5A). Quantitative analysis of the western blots revealed that treatment with RANKL significantly increased the phosphorylation of ERK, JNK and p38 compared with the control group (Fig. 5B). This phosphorylation was significantly enhanced by co-treatment with RANKL and APLN. To determine whether APLN promoted osteoclast differentiation through MAPK

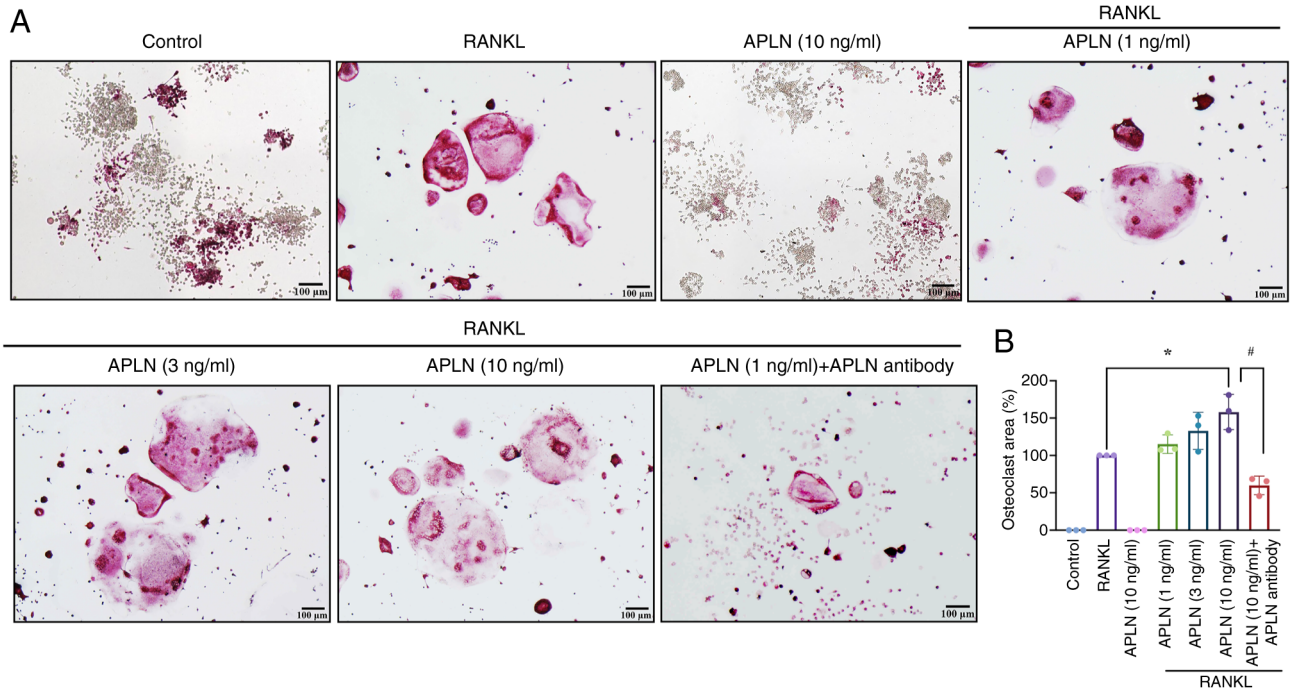

Figure 1. APLN promotes RANKL-induced osteoclast differentiation. RAW264.7 cells were treated with RANKL (50 ng/ml) in the presence or absence of APLN (1, 3 or 10 ng/ml) for 5 days. (A) Representative images of cells were stained with tartrate-resistant acid phosphatase to identify mature osteoclasts. (B) Quantification of the osteoclast area percentage using ImageJ software. Scale bar, 100 μm. *P<0.05 vs. RANKL-treated group. #P<0.05 vs. RANKL + APLN (10 ng/ml)-treated group. RANKL, receptor activator of NF-κB ligand; APLN, apelin.

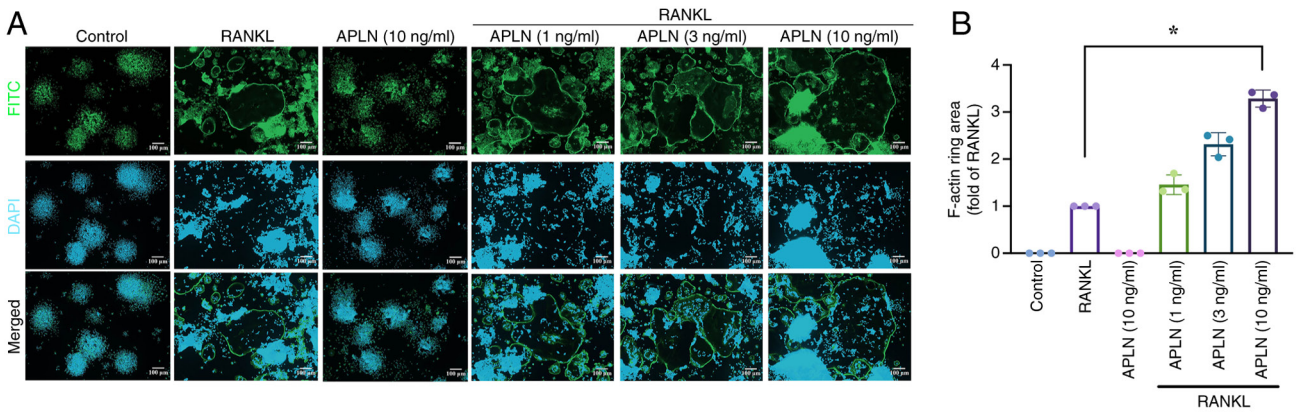

Figure 2. APLN enhances F-actin ring formation in RANKL-treated RAW264.7 cells. (A) Immunofluorescence staining of F-actin (green, Alexa Fluor 488) and nuclei (blue, DAPI) in RAW264.7 cells treated with RANKL (50 ng/ml) and various concentrations of apelin (1, 3 or 10 ng/ml) for 5 days. Merged images are also shown. (B) Quantification of F-actin ring area relative to the RANKL-treated group. Scale bar, 100 μm. *P<0.05 vs. RANKL-treated group. RANKL, receptor activator of NF-κB ligand; APLN, apelin.

pathway activation, the effects of selective MAPK inhibitors on APLN-treated cells were assessed. RAW264.7 cells were treated with APLN and RANKL in the presence of the ERK inhibitor FR180294, JNK inhibitor SP600125 or p38 inhibitor SB203580, and the expression levels of osteoclast marker genes were subsequently assessed by RT-qPCR analysis. As expected, treatment with RANKL and APLN significantly upregulated the mRNA expression levels of ACP5, CTSK, MMP9 and NFATc1 compared with those in the control group. However, this enhanced expression was significantly suppressed upon treatment with MAPK inhibitors (Fig. 5C), indicating that the activation of MAPK signaling was important for APLN activity in promoting RANKL-mediated osteoclast differentiation.

The present study then investigated the role of NF-κB signaling in APLN-enhanced RANKL-induced osteoclastogenesis. Western blot analysis and signal semi-quantification revealed that RANKL treatment significantly increased the phosphorylation of IKK, IκB and NF-κB p65 compared with that in the control group. Co-treatment with APLN and RANKL significantly enhanced the phosphorylation levels of these proteins relative to RANKL alone (Fig. 6A and B). Consistently, luciferase reporter assays revealed that APLN significantly enhanced RANKL-induced NF-κB transcriptional activity (Fig. 6C). In addition, RT-qPCR analysis demonstrated that co-treatment of RAW264.7 cells with APLN and RANKL significantly upregulated the expression

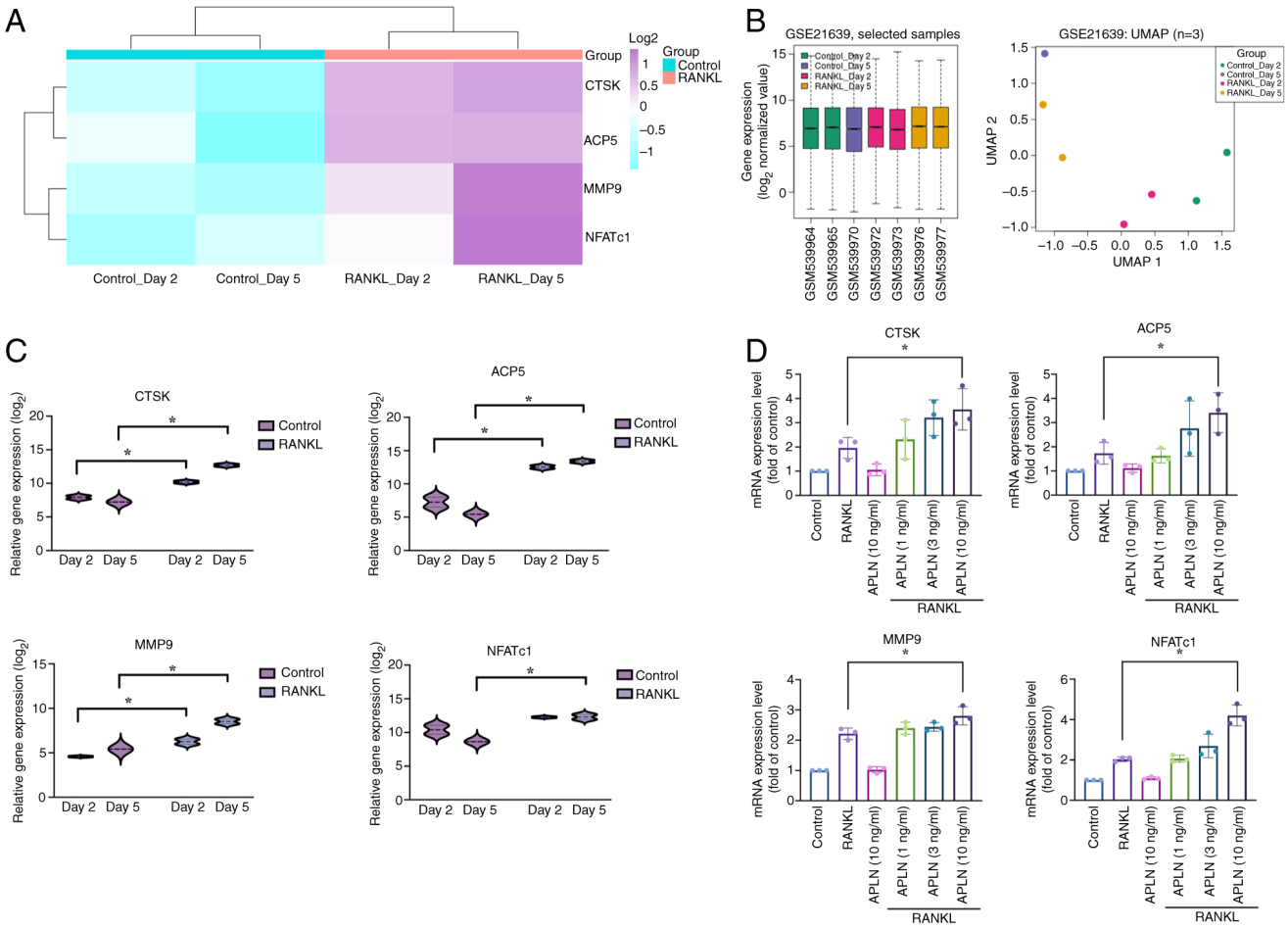

Figure 3. APLN enhances osteoclast marker gene expression under RANKL stimulation. (A) Heatmap analysis of osteoclast-related gene expression (ACP5, CTSK, MMP9 and NFATc1) from the GSE21639 dataset. RAW264.7 cells were treated with or without RANKL for 2 or 5 days. (B) Boxplot and UMAP analyses of the GSE21639 dataset. The boxplot shows consistent overall gene expression distributions across all samples without outliers, while the UMAP plot illustrates the clustering of samples according to experimental conditions (Control or RANKL treatment on days 2 and 5). These analyses were conducted to assess dataset quality and comparability prior to differential expression analysis. (C) Violin plot visualization of the transcript levels of each gene. Data were $\log_2$-transformed and grouped by treatment condition. (D) RAW264.7 cells were treated with RANKL (50 ng/ml) and increasing concentrations of APLN (1, 3 or 10 ng/ml) for 5 days. The mRNA expression of osteoclast markers was determined using reverse transcription-quantitative PCR. *P<0.05 vs. RANKL-treated group. UMAP, uniform manifold approximation and projection analyses; RANKL, receptor activator of NF-κB ligand; APLN, apelin; ACP5, acid phosphatase 5, tartrate resistant; CTSK, cathepsin K; MMP9, matrix metalloproteinase 9; NFATc1, nuclear factor of activated T-cells 1.

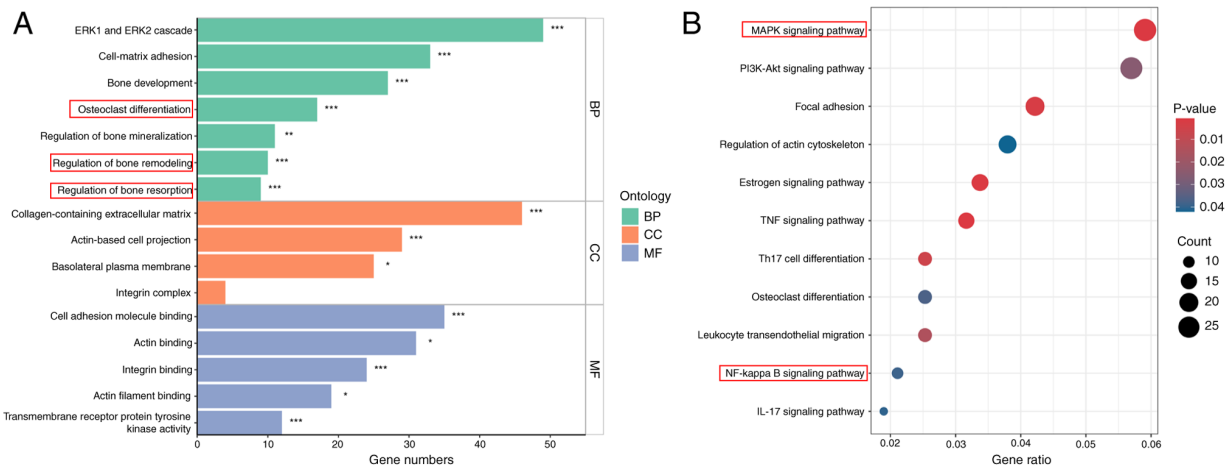

Figure 4. Transcriptome enrichment analysis identifies osteoclast-related signaling pathways activated by RANKL. DEGs were identified from the GSE21639 dataset by comparing RANKL-treated and control RAW264.7 cells on day 5 ($|\log_2$ fold change$|$>2, P<0.05). (A) Gene Ontology enrichment analysis of upregulated DEGs revealed significant enrichment in BP, CC and MF terms. (B) Kyoto Encyclopedia of Genes and Genomes pathway analysis revealed the significant enrichment of the 'NF-kappa B signaling pathway' and 'MAPK signaling pathway'. Adjusted P<0.05 was considered to indicate a significant difference. *P<0.05, **P<0.01 and ***P<0.001. DEGs, differentially expressed genes; BP, biological process; CC, cellular component; MF, molecular function; RANKL, receptor activator of NF-κB ligand.

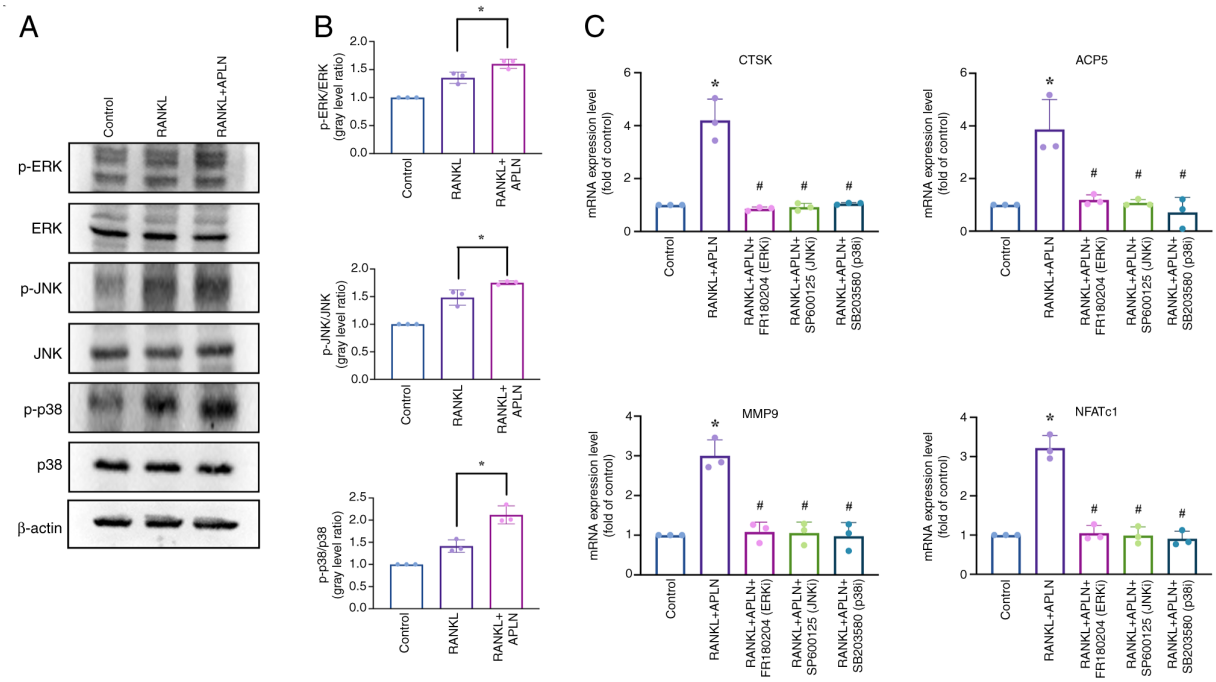

Figure 5. APLN promotes osteoclast differentiation through activation of the MAPK pathway. (A) RAW264.7 cells were exposed to a control medium, RANKL (50 ng/ml) or RANKL + APLN (10 ng/ml) for 10 min. Cell lysates were subjected to western blot analysis to assess the phosphorylation of MAPK family members, including ERK, JNK and p38. (B) Signal intensities of p-ERK, p-JNK and p-p38 were semi-quantified using ImageJ software and normalized to their respective total protein levels. *P<0.05 vs. RANKL-treated group. (C) mRNA expression levels of osteoclast marker genes (ACP5, CTSK, MMP9 and NFATc1) were assessed using reverse transcription-quantitative PCR in cells treated with RANKL + APLN (10 ng/ml), either alone or in combination with MAPK inhibitors (FR180204 for ERK, SP600125 for JNK and SB203580 for p38). *P<0.05 vs. Control group; #P<0.05 vs. RANKL + APLN group. APLN, apelin; RANKL, receptor activator of NF-κB ligand; ACP5, acid phosphatase 5, tartrate resistant; CTSK, cathepsin K; MMP9, matrix metalloproteinase 9; NFATc1, nuclear factor of activated T-cells 1; p-, phosphorylated-; ERK/JNK/p38i, ERK/JNK/p38 inhibitor.

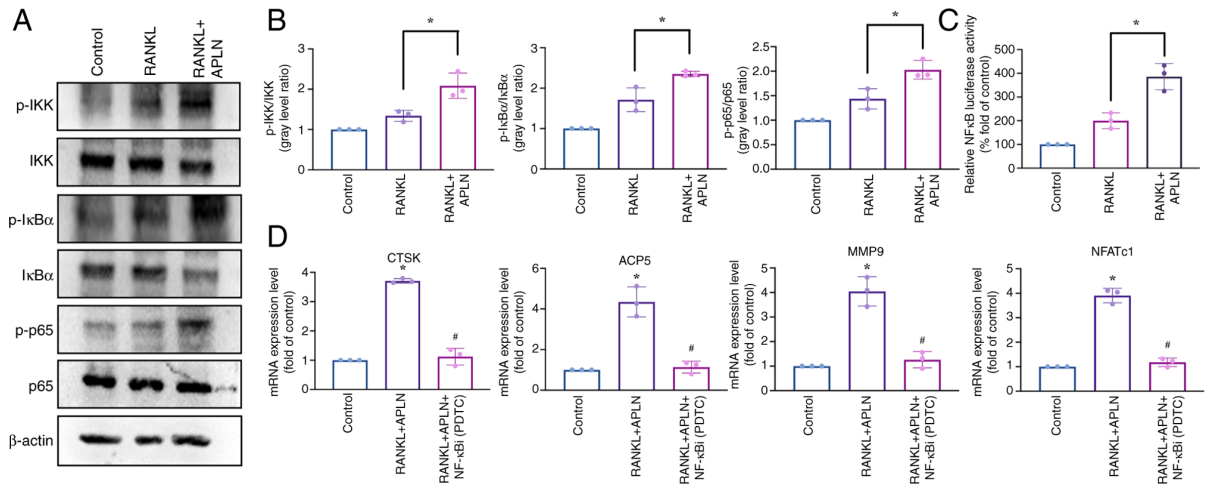

Figure 6. APLN enhances RANKL-induced activation of the NF-κB signaling pathway. (A) Western blot analysis of RAW264.7 cells treated with control medium, RANKL (50 ng/ml) or RANKL + APLN (10 ng/ml) for 10 min. Protein levels of p-IKK, p-IκB and p-p65 were detected to evaluate pathway activation. (B) Semi-quantification of p-IKK, p-IκB and p-p65 levels relative to their corresponding total proteins was performed using ImageJ software. (C) RAW264.7 cells were transfected with an NF-κB luciferase reporter construct and treated with RANKL (50 ng/ml) or RANKL + APLN (10 ng/ml) for 24 h. Luciferase activity was measured using cell lysates and reporter buffer mixed at a 1:1 ratio. NF-κB transcriptional activity is shown as the fold change relative to the RANKL-only group. *P<0.05 vs. RANKL-treated group. (D) Reverse transcription-quantitative PCR analysis of osteoclast marker genes (ACP5, CTSK, MMP9 and NFATc1) in cells treated with RANKL + APLN (10 ng/ml) with or without the NF-κBi PDTC (20 μM). *P<0.05 vs. Control group; #P<0.05 vs. RANKL + APLN group. APLN, apelin; RANKL, receptor activator of NF-κB ligand; ACP5, acid phosphatase 5, tartrate resistant; CTSK, cathepsin K; MMP9, matrix metalloproteinase 9; NFATc1, nuclear factor of activated T-cells 1; p-, phosphorylated-; NF-κBi, NF-κB inhibitor; PDTC, pyrrolidinedithiocarbamate ammonium.

of osteoclast marker genes compared with the control group; however, this effect was significantly reduced by the NF-κB inhibitor PDTC (Fig. 6D). Taken together, these results suggested that APLN may promote RANKL-mediated osteoclast differentiation by activating the MAPK and NF-κB signaling pathways.

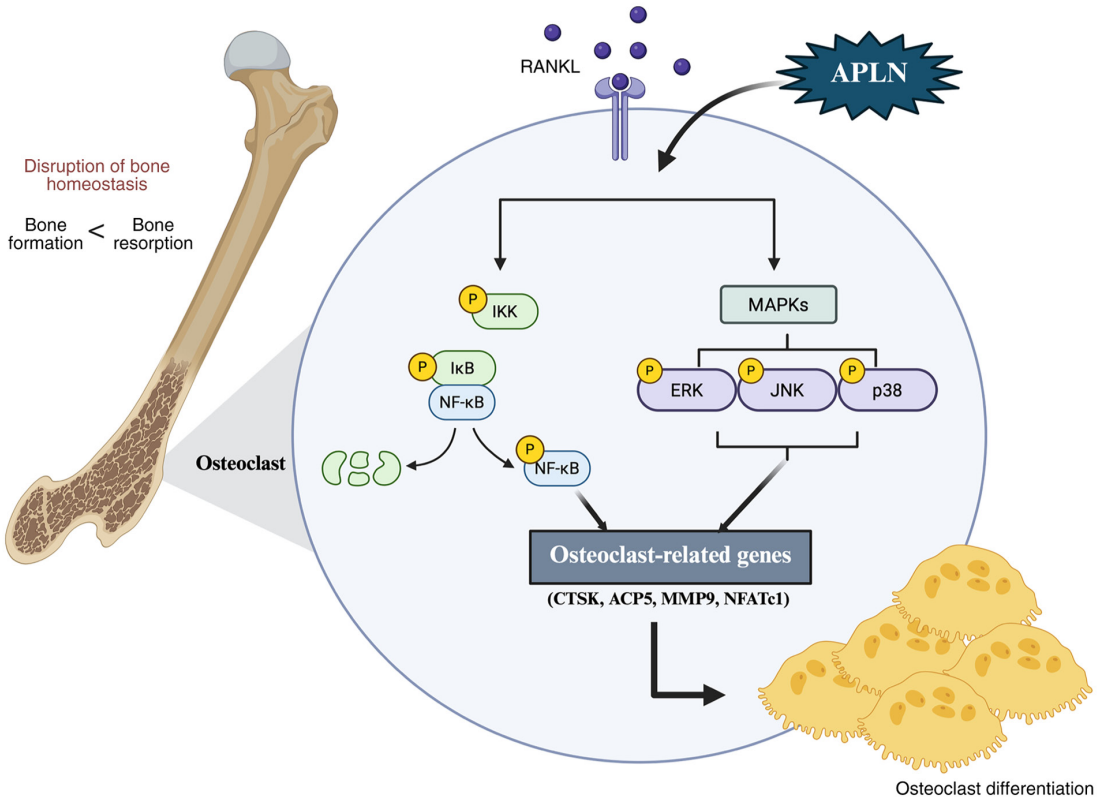

Figure 7. APLN promotes RANKL-mediated osteoclastogenesis, and activates MAPK and NF-κB signaling pathways. APLN augmented RANKL-induced phosphorylation of ERK, JNK, p38 and NF-κB p65, leading to the increased expression of osteoclast marker genes and enhanced osteoclast differentiation and function. APLN, apelin; RANKL, receptor activator of NF-κB ligand; ACP5, acid phosphatase 5, tartrate resistant; CTSK, cathepsin K; MMP9, matrix metalloproteinase 9; NFATc1, nuclear factor of activated T-cells 1.

Discussion

Adipokines are bioactive peptides derived from adipose tissue that regulate key physiological processes, including metabolism, inflammation and vascular function. Increasing evidence has indicated that adipokines exert effects on the musculoskeletal system and also participate in the regulation of bone remodeling (27,28). Leptin has been shown to induce the production of oncostatin M in human osteoblasts, thereby promoting inflammatory signaling that disrupts osteoblast function and bone homeostasis (29). The proinflammatory and catabolic effects of visfatin in gingival fibroblasts may indirectly promote osteoclast activation, thereby exacerbating alveolar bone resorption in periodontitis (30). However, the roles of numerous adipokines in bone homeostasis remain yet to be fully elucidated. APLN has been identified as an adipokine implicated in cardiovascular control, glucose metabolism and inflammatory responses (31-33). Despite its broad biological role, information on the influence of APLN on osteoclast differentiation or bone resorption is limited.

The present study demonstrated that APLN enhanced RANKL-induced osteoclast differentiation and function in a concentration-dependent manner. Co-treatment with APLN significantly increased TRAP-positive multinucleated cell formation, F-actin ring size and the expression of osteoclast marker genes, including ACP5, CTSK, MMP9 and NFATc1. These findings provided novel insights into the bone-regulatory role of APLN and suggested that APLN inhibition may serve as a potential strategy to modulate osteoclast function.

Bone remodeling is a dynamic process that requires regulation to maintain a balance between osteoblast-mediated bone formation and osteoclast-mediated bone resorption (1). The disruption of this balance, particularly when bone resorption outpaces formation, contributes to the pathogenesis of various skeletal disorders, including osteoporosis, rheumatoid arthritis and periodontitis (34-36). Osteoclast differentiation and activation are primarily driven by RANKL, which initiates a cascade of intracellular signaling events upon binding to its receptor RANK on osteoclast precursors (37). Activated pathways include the NF-κB and MAPK pathways, both of which are important for the induction of key osteoclastogenic transcription factors such as NFATc1 (38). The present study found that APLN co-treatment with RANKL significantly enhanced the phosphorylation of ERK, JNK and p38 in the MAPK pathway, as well as IKK, IκB and NF-κB p65 in the canonical NF-κB pathway. The inhibition of these signaling pathways significantly attenuated the APLN-induced upregulation of osteoclast-specific genes, indicating that APLN promoted osteoclastogenesis through the activation of classical signaling cascades downstream of RANKL. These findings suggested that APLN may facilitate pathological bone resorption by amplifying RANKL-induced signals.

Building on these mechanistic insights, targeting APLN may represent a promising therapeutic strategy for osteolytic conditions such as osteoporosis, rheumatoid arthritis and

periodontitis. However, given that APLN is a multifunctional adipokine involved in cardiovascular regulation, angiogenesis and metabolic homeostasis, systemic inhibition may lead to undesirable off-target effects (39-42). To overcome these limitations, localized treatment strategies may offer a more favorable therapeutic strategy. For example, APLN-silencing molecules, such as small interfering RNAs or miRNA mimics, could be encapsulated within engineered exosomes for targeted delivery to the bone microenvironment. This approach may enable site-specific suppression of APLN activity, thereby attenuating osteoclast overactivation while minimizing systemic effects. Further investigations are warranted to evaluate the feasibility and therapeutic benefit of exosome-mediated APLN inhibition in bone-resorptive diseases.

Current pharmacological approaches for the treatment of bone-resorptive diseases mainly focus on inhibiting osteoclast activity (43). Bisphosphonates, such as alendronate and zoledronic acid, are used to suppress osteoclast-mediated bone resorption by inducing osteoclast apoptosis (44). While effective in reducing fracture risk, their prolonged use has been shown to be associated with complications such as atypical femoral fractures and osteonecrosis of the jaw (45). Denosumab, a monoclonal antibody against RANKL, provides the potent and reversible suppression of osteoclastogenesis, but its discontinuation may lead to rapid bone loss and an increased risk of multiple vertebral fractures (46). Furthermore, both treatments broadly suppress bone turnover, potentially impairing the physiological remodeling process.

Other anti-resorptive agents, including calcitonin, hormone replacement therapy (HRT) and SERMs such as raloxifene, have also been used in clinical practice. However, these options are limited by suboptimal efficacy and potential systemic risks. For example, calcitonin has been associated with an increased risk of developing cancer (47); and HRT has been a subject of concern regarding cardiovascular disease and hormone-sensitive cancers (48). In addition, SERMs may increase the risk of thromboembolism (49). Given these limitations, there is growing interest in identifying novel osteoclastogenic regulatory pathways complementing current therapies. A co-therapeutic strategy combining adipokine-targeted interventions with current anti-resorptive agents may improve outcomes in osteolytic disease treatment.

In conclusion, the present study demonstrated that APLN may promote RANKL-induced osteoclast differentiation and function, and upregulate the levels of key osteoclast marker genes. APLN was found to enhance the MAPK and NF-κB signaling pathways in the presence of RANKL, and the inhibition of these pathways attenuated the ability of APLN to promote osteoclast differentiation (Fig. 7). These findings provide a novel perspective into the role of APLN in bone remodeling and identify APLN as an important enhancer of osteoclastogenesis. Given these observations, therapeutic strategies aimed at inhibiting APLN signaling may represent a novel approach for mitigating pathological bone resorption in conditions such as osteoporosis, inflammatory arthritis and periodontitis.

Acknowledgements

Not applicable.

Funding

The authors acknowledge financial support from the Ministry of Science and Technology of Taiwan (grant nos. MOST 110-2320-B-039-022-MY3, NSTC 112-2320-B-039-035-MY3, MOST 111-2314-B-039-048-MY3, NSTC 113-2320-B-039-049-MY3, NSTC 111-2320-B-371-002, NSTC 114-2314-B-039-051-MY3 and NSTC 114-2320-B-039-016-), the China Medical University Hospital (grant nos. DMR-114-003 and DMR-114-043) and the China Medical University (grant no. CMU 113-ASIA-05).

Availability of data and materials

The data generated in the present study may be requested from the corresponding author.

Authors' contributions

YHW, YYW, CHTs, and CHTa contributed to the conception and design of the study. YCF, CYK and HTC were responsible for data acquisition and experimental validation. CHTs and YYL contributed to data analysis and interpretation. YHW and CHTa drafted the manuscript and confirm the authenticity of all the raw data. All authors critically revised the manuscript for important intellectual content and agreed to be accountable for all aspects of the work. All authors read and approved the final manuscript.

Ethics approval and consent to participate

Not applicable.

Patient consent for publication

Not applicable.

Competing interests

The authors declare that they have no competing interests.

References

1. Bolamperti S, Villa I and Rubinacci A: Bone remodeling: An operational process ensuring survival and bone mechanical competence. Bone Res 10: 48, 2022.
2. Zhu L, Zhou C, Chen S, Huang D, Jiang Y, Lan Y, Zou S and Li Y: Osteoporosis and alveolar bone health in periodontitis niche: A predisposing factors-centered review. Cells 11: 3380, 2022.
3. Ashai S and Harvey NC: Rheumatoid arthritis and bone health. Clin Med (Lond) 20: 565-567, 2020.
4. Park JJ and Wong C: Pharmacological prevention and management of skeletal-related events and bone loss in individuals with cancer. Semin Oncol Nurs 38: 151276, 2022.
5. Salari N, Ghasemi H, Mohammadi L, Behzadi MH, Rabieenia E, Shohaimi S and Mohammadi M: The global prevalence of osteoporosis in the world: A comprehensive systematic review and meta-analysis. J Orthop Surg Res 16: 609, 2021.
6. Elahmer NR, Wong SK, Mohamed N, Alias E, Chin KY and Muhammad N: Mechanistic insights and therapeutic strategies in osteoporosis: A comprehensive review. Biomedicines 12: 1635, 2024.
7. Ayers C, Kansagara D, Lazur B, Fu R, Kwon A and Harrod C: Effectiveness and safety of treatments to prevent fractures in people with low bone mass or primary osteoporosis: A living systematic review and network meta-analysis for the American College of Physicians. Ann Intern Med 176: 182-195, 2023.

8. Weivoda MM and Bradley EW: Macrophages and bone remodeling. J Bone Miner Res 38: 359-369, 2023.
9. Campbell MJ, Bustamante-Gomez C, Fu Q, Beenken KE, Reyes-Pardo H, Smeltzer MS and O'Brien CA: RANKL-mediated osteoclast formation is required for bone loss in a murine model of Staphylococcus aureus osteomyelitis. Bone 187: 117181, 2024.
10. Park JH, Lee NK and Lee SY: Current understanding of RANK signaling in osteoclast differentiation and maturation. Mol Cells 40: 706-713, 2017.
11. Yan J, Wang A, Cao J and Chen L: Apelin/APJ system: An emerging therapeutic target for respiratory diseases. Cell Mol Life Sci 77: 2919-2930, 2020.
12. Wang YH, Kuo SJ, Liu SC, Wang SW, Tsai CH, Fong YC and Tang CH: Apelin affects the progression of osteoarthritis by regulating VEGF-dependent angiogenesis and miR-150-5p expression in human synovial fibroblasts. Cells 9: 594, 2020.
13. Hu G, Wang Z, Zhang R, Sun W and Chen X: The role of apelin/apelin receptor in energy metabolism and water homeostasis: A comprehensive narrative review. Front Physiol 12: 632886, 2021.
14. Chapman FA, Melville V, Godden E, Morrison B, Bruce L, Maguire JJ, Davenport AP, Newby DE and Dhaun N: Cardiovascular and renal effects of apelin in chronic kidney disease: A randomised, double-blind, placebo-controlled, crossover study. Nat Commun 15: 8387, 2024.
15. Wysocka MB, Pietraszek-Gremplewicz K and Nowak D: The role of apelin in cardiovascular diseases, obesity and cancer. Front Physiol 9: 557, 2018.
16. Chang TK, Wang YH, Kuo SJ, Wang SW, Tsai CH, Fong YC, Wu NL, Liu SC and Tang CH: Apelin enhances IL-1beta expression in human synovial fibroblasts by inhibiting miR-144-3p through the PI3K and ERK pathways. Aging (Albany NY) 12: 9224-9239, 2020.
17. Ducy P, Amling M, Takeda S, Priemel M, Schilling AF, Beil FT, Shen J, Vinson C, Rueger JM and Karsenty G: Leptin inhibits bone formation through a hypothalamic relay: A central control of bone mass. Cell 100: 197-207, 2000.
18. Tu Q, Zhang J, Dong LQ, Saunders E, Luo E, Tang J and Chen J: Adiponectin inhibits osteoclastogenesis and bone resorption via APPL1-mediated suppression of Akt1. J Biol Chem 286: 12542-12553, 2011.
19. Wattanachanya L, Lu WD, Kundu RK, Wang L, Abbott MJ, O'Carroll D, Quertermous T and Nissenson RA: Increased bone mass in mice lacking the adipokine apelin. Endocrinology 154: 2069-2080, 2013.
20. Izgut-Uysal VN, Gemici B, Birsen I, Acar N and Ustunel I: The effect of apelin on the functions of peritoneal macrophages. Physiol Res 66: 489-496, 2017.
21. Sharma P, Patntirapong S, Hann S and Hauschka PV: RANKL-RANK signaling regulates expression of xenotropic and polytropic virus receptor (XPR1) in osteoclasts. Biochem Biophys Res Commun 399: 129-132, 2010.
22. Love MI, Huber W and Anders S: Moderated estimation of fold change and dispersion for RNA-seq data with DESeq2. Genome Biol 15: 550, 2014.
23. Dennis G Jr, Sherman BT, Hosack DA, Yang J, Gao W, Lane HC and Lempicki RA: DAVID: Database for annotation, visualization, and integrated discovery. Genome Biol 4: P3, 2003.
24. Livak KJ and Schmittgen TD: Analysis of relative gene expression data using real-time quantitative PCR and the 2(-Delta Delta C(T)) method. Methods 25: 402-408, 2001.
25. Lampiasi N, Russo R, Kireev I, Strelkova O, Zhironkina O and Zito F: Osteoclasts differentiation from murine RAW 264.7 cells stimulated by RANKL: Timing and behavior. Biology (Basel) 10: 117, 2021.
26. Sun W, Li Y, Li J, Tan Y, Yuan X, Meng H, Ye J, Zhong G, Jin X, Liu Z, *et al*: Mechanical stimulation controls osteoclast function through the regulation of Ca(2+)-activated Cl(-) channel Anoctamin 1. Commun Biol 6: 407, 2023.
27. Greco EA, Lenzi A and Migliaccio S: The obesity of bone. Ther Adv Endocrinol Metab 6: 273-286, 2015.
28. Armutcu F, McCloskey E and Ince M: Obesity significantly modifies signaling pathways associated with bone remodeling and metabolism. J Cell Signal 5: 183-194, 2024.
29. Yang WH, Tsai CH, Fong YC, Huang YL, Wang SJ, Chang YS and Tang CH: Leptin induces oncostatin M production in osteoblasts by downregulating miR-93 through the Akt signaling pathway. Int J Mol Sci 15: 15778-15790, 2014.
30. Park KH, Kim DK, Huh YH, Lee G, Lee SH, Hong Y, Kim SH, Kook MS, Koh JT, Chun JS, *et al*: NAMPT enzyme activity regulates catabolic gene expression in gingival fibroblasts during periodontitis. Exp Mol Med 49: e368, 2017.
31. de Oliveira AA, Vergara A, Wang X, Vederas JC and Oudit GY: Apelin pathway in cardiovascular, kidney, and metabolic diseases: Therapeutic role of apelin analogs and apelin receptor agonists. Peptides 147: 170697, 2022.
32. Wang Q, Wang B, Zhang W, Zhang T, Liu Q, Jiao X, Ye J, Hao Y, Gao Q, Ma G, *et al*: APLN promotes the proliferation, migration, and glycolysis of cervical cancer through the PI3K/AKT/mTOR pathway. Arch Biochem Biophys 755: 109983, 2024.
33. Chen L, Tao Y and Jiang Y: Apelin activates the expression of inflammatory cytokines in microglial BV2 cells via PI-3K/Akt and MEK/Erk pathways. Sci China Life Sci 58: 531-540, 2015.
34. Tilotta F, Gosset M, Herrou J, Briot K and Roux C: Association between osteoporosis and periodontitis. Joint Bone Spine 92: 105883, 2025.
35. Llorente I, Garcia-Castaneda N, Valero C, Gonzalez-Alvaro I and Castaneda S: Osteoporosis in rheumatoid arthritis: Dangerous liaisons. Front Med (Lausanne) 7: 601618, 2020.
36. Sarhan RS, El-Hammady AM, Marei YM, Elwia SK, Ismail DM and Ahmed EAS: Plasma levels of miR-21b and miR-146a can discriminate rheumatoid arthritis diagnosis and severity. Biomedicine (Taipei) 15: 30-41, 2025.
37. Takegahara N, Kim H and Choi Y: Unraveling the intricacies of osteoclast differentiation and maturation: Insight into novel therapeutic strategies for bone-destructive diseases. Exp Mol Med 56: 264-272, 2024.
38. Lee NK: RANK signaling pathways and key molecules inducing osteoclast differentiation. Biomed Sci Lett 23: 295-302, 2017.
39. Castan-Laurell I, Dray C and Valet P: The therapeutic potentials of apelin in obesity-associated diseases. Mol Cell Endocrinol 529: 111278, 2021.
40. Yasir M, Senthilkumar GP, Jayashree K, Ramesh Babu K, Vadivelan M and Palanivel C: Association of serum omentin-1, apelin and chemerin concentrations with the presence and severity of diabetic retinopathy in type 2 diabetes mellitus patients. Arch Physiol Biochem 128: 313-320, 2022.
41. Gao S and Chen H: Therapeutic potential of apelin and Elabela in cardiovascular disease. Biomed Pharmacother 166: 115268, 2023.
42. Couvineau P and Llorens-Cortes C: Metabolically stable apelin analogs: Development and functional role in water balance and cardiovascular function. Clin Sci (Lond) 139: 131-149, 2025.
43. Liang B, Burley G, Lin S and Shi YC: Osteoporosis pathogenesis and treatment: Existing and emerging avenues. Cell Mol Biol Lett 27: 72, 2022.
44. Mbese Z and Aderibigbe BA: Bisphosphonate-based conjugates and derivatives as potential therapeutic agents in osteoporosis, bone cancer and metastatic bone cancer. Int J Mol Sci 22: 6869, 2021.
45. Hussain MA, Joseph A, Cherian VM, Srivastava A, Cherian KE, Kapoor N and Paul TV: Bisphosphonate-induced atypical femoral fracture in tandem: long-term follow-up is warranted. Endocrinol Diabetes Metab Case Rep 2022: 2022:22-0249, 2022.
46. Tsourdi E, Zillikens MC, Meier C, Body JJ, Rodriguez EG, Anastasilakis AD, Abrahamsen B, McCloskey E, Hofbauer LC, Guañabens N, *et al*: Fracture risk and management of discontinuation of denosumab therapy: A systematic review and position statement by ECTS. J Clin Endocrinol Metab 26: dgaa756, 2020.
47. Okamoto H, Shibazaki N, Yoshimura T, Uzawa T and Sugimoto T: Association between elcatonin use and cancer risk in Japan: A follow-up study after a randomized, double-blind, placebo-controlled study of once-weekly elcatonin in primary postmenopausal osteoporosis. Osteoporos Sarcopenia 6: 15-19, 2020.
48. Vinogradova Y, Coupland C and Hippisley-Cox J: Use of hormone replacement therapy and risk of breast cancer: Nested case-control studies using the QResearch and CPRD databases. BMJ 371: m3873, 2020.
49. Nordstrom BL, Cai B, De Gregorio F, Ban L, Fraeman KH, Yoshida Y and Gibbs T: Risk of venous thromboembolism among women receiving ospemifene: A comparative observational study. Ther Adv Drug Saf: Nov 19, 2022 (Epub ahead of print).